

Unleashing the Power of Contrastive Self-Supervised Visual Models via Contrast-Regularized Fine-Tuning

Yifan Zhang¹ Bryan Hooi¹ Dapeng Hu¹ Jian Liang¹ Jiashi Feng¹

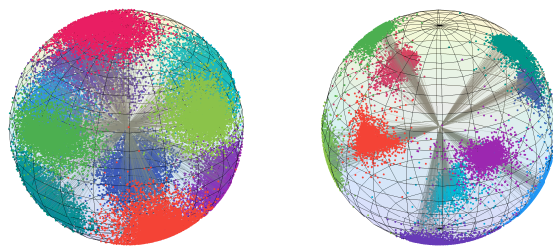
Abstract

Contrastive self-supervised learning (CSL) leverages unlabeled data to train models that provide instance-discriminative visual representations uniformly scattered in the feature space. In deployment, the common practice is to directly fine-tune models with the cross-entropy loss, which however may not be an optimal strategy. Although cross-entropy tends to separate inter-class features, the resulted models still have limited capability of reducing intra-class feature scattering that inherits from pre-training, and thus may suffer unsatisfactory performance on downstream tasks. In this paper, we investigate whether applying contrastive learning to fine-tuning would bring further benefits, and analytically find that optimizing the supervised contrastive loss benefits both class-discriminative representation learning and model optimization during fine-tuning. Inspired by these findings, we propose Contrast-regularized tuning (Core-tuning), a novel approach for fine-tuning contrastive self-supervised visual models. Instead of simply adding the contrastive loss to the objective of fine-tuning, Core-tuning also generates hard sample pairs for more effective contrastive learning through a novel feature mixup strategy, as well as improves the generalizability of the model by smoothing the decision boundary via mixed samples. Extensive experiments on image classification and semantic segmentation verify the effectiveness of Core-tuning.

1. Introduction

Pre-training a deep neural network on a large database and then fine-tuning it on downstream tasks has been a popular scheme in the machine learning community. Recently, contrastive self-supervised learning (CSL) has attracted much

¹National University of Singapore. Correspondence to: Yifan Zhang <yifan.zhang@u.nus.edu>, Jiashi Feng <elefjia@nus.edu.sg>.



(a) Training with \mathcal{L}_{ce} (b) Training with $\mathcal{L}_{ce} + \mathcal{L}_{con}$

Figure 1. Visualizations of learned features by ResNet-18 on the CIFAR10 validation set. Compared to training with only cross-entropy \mathcal{L}_{ce} , the contrastive loss \mathcal{L}_{con} helps regularize the feature space and makes it more discriminative. Best viewed in color.

attention (He et al., 2020; Chen et al., 2020a;b). CSL leverages unlabeled data to train a visual model via contrastive learning, which maximizes the feature similarity for two augmentations of the same instance and minimizes the similarity of two instances (Wu et al., 2018). The learned model is able to provide instance-discriminative visual representations that are uniformly scattered in the feature space (Wang & Isola, 2020). When deploying the model, the common practice is to directly fine-tune it with the cross-entropy loss (Ericsson et al., 2020).

However, fine-tuning with only cross-entropy may not be an optimal strategy. Although cross-entropy tends to learn separable features among classes, the resulted model is still limited in the capability of reducing intra-class feature scattering (Liu et al., 2016; Wen et al., 2016) that inherits from pre-training, and thus may suffer unsatisfactory performance on downstream tasks. Meanwhile, despite substantial CSL studies on model pre-training (Tian et al., 2020; Kalantidis et al., 2020), few have explored the fine-tuning process. In this work, we explore how to better fine-tune contrastive self-supervised visual models on downstream tasks.

Considering that optimizing the unsupervised contrastive loss during pre-training yields models with instance-level discriminative power, we investigate whether applying contrastive learning to fine-tuning would bring further benefits. To answer this, we analyze the contrastive loss during fine-tuning (see Section 3) and find that it offers two benefits. First, integrating the contrastive loss into cross-entropy can provide an additional regularization effect as compared to

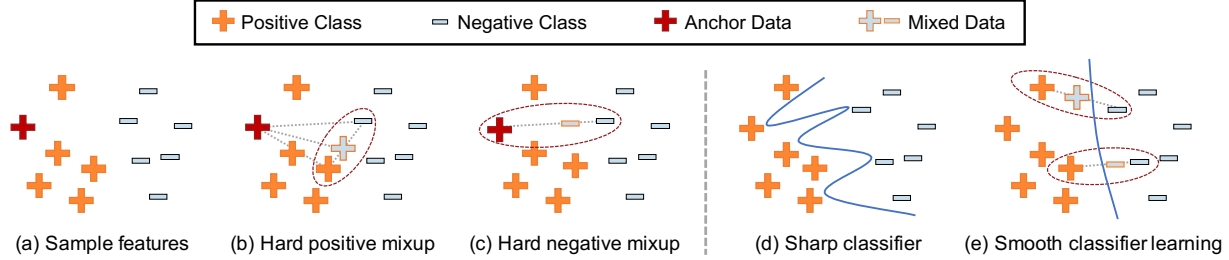


Figure 2. Illustration of two challenges in contrastive fine-tuning. (1) How to mine hard sample pairs for more effective contrastive fine-tuning. As shown in (a), the majority of sample features are easy-to-contrast, and may induce negligible contrastive loss gradients that contribute little to learning more discriminative features. To address this, Core-tuning generates both (b) hard positive pairs and (c) hard negative pairs via feature mixup. (2) How to improve the generalizability of the model. As shown in (d), no matter whether features are discriminative, training with cross-entropy often results in a sharp decision boundary near training data, leading to limited generalization performance. To enhance generalizability, Core-tuning further smooths the decision boundary via the mixed data, as shown in (e).

cross-entropy based fine-tuning for class-discriminative representation learning. Such an effect encourages the model to learn a low-entropy feature cluster for each class (*i.e.*, high intra-class compactness) and a high-entropy feature space (*i.e.*, large inter-class separation degree). See feature visualization on CIFAR10 in Figure 1 for an illustration. Second, optimizing the contrastive loss will minimize the infimum of the cross-entropy loss over training data, which can provide an additional optimization effect for model training during fine-tuning. Based on the optimization effectiveness as well as the regularization effectiveness on features, we argue that optimizing the contrastive loss during fine-tuning can further improve model performance on downstream tasks.

We thus propose a contrast-regularized tuning approach, termed Core-tuning, to fine-tune contrastive self-supervised models and enhance their performance on downstream tasks, where a contrastive regularizer is applied to make the model more class-discriminative. Instead of simply adding the contrastive loss to the objective of fine-tuning (Gunel et al., 2021), Core-tuning further applies two novel designs. First, Core-tuning generates hard sample pairs for more effective contrastive learning via a new feature mixup strategy. Concretely, as shown in Figure 2 (a), the majority of sample features are easy-to-contrast (Harwood et al., 2017), and may produce negligible contrastive loss gradients that contribute little to learning more discriminative representations. To address this, Core-tuning mixes the learned features to generate both hard positive and hard negative pairs for each anchor data (See Figure 2 (b-c)). Here, hard positives indicate the positive pairs far away from the anchor, while hard negatives are the negative pairs close to the anchor. Meanwhile, since hard positive pairs are more informative for contrastive learning (Harwood et al., 2017), Core-tuning assigns higher importance weights to them in contrastive fine-tuning. Second, Core-tuning seeks to improve model generalizability by smoothing the decision boundary. As shown in Figure 2 (d), the decision boundary trained with cross-entropy is often sharp and close to training data (Verma et al., 2019), which may lead to incor-

rect yet confident predictions when evaluated on slightly different test samples. Inspired by (Verma et al., 2019) in which mixed data are used to help learn smoother decision boundaries, Core-tuning further uses the mixed features to train the classifier (See Figure 2 (e)).

Extensive experiments on image classification and semantic segmentation verify the effectiveness of Core-tuning. We also empirically find that Core-tuning benefits contrastive self-supervised models in terms of domain generalization and adversarial robustness on downstream tasks.

The main contributions of this paper are threefold. 1) To our best knowledge, we are among the first to look into the fine-tuning stage of contrastive self-supervised visual models and propose a novel contrast-regularized tuning method. 2) We theoretically analyze the benefits of the supervised contrastive loss on representation learning and model optimization, and reveal that it is beneficial to model fine-tuning. 3) We empirically demonstrate that Core-tuning can effectively improve the fine-tuning performance of contrastive self-supervised models on many downstream tasks. Considering the theoretical guarantee and empirical effectiveness of Core-tuning, we recommend using it as a standard baseline to fine-tune contrastive self-supervised models.

2. Related Work

Contrastive self-supervised learning (CSL). Self-supervised learning is a kind of unsupervised representation learning method based on self-supervised proxy tasks, *e.g.*, rotation prediction (Gidaris et al., 2018) and colorization prediction (Larsson et al., 2016). Recently, CSL has become the most popular self-supervised paradigm, which treats each instance as a category to learn instance-discriminative representations. State-of-the-art CSL methods include InsDis (Wu et al., 2018), MoCo (He et al., 2020), SimCLR (Chen et al., 2020a;b) and InfoMin (Tian et al., 2020). Most CSL studies are devoted to network pre-training, but few have explored the fine-tuning process.

As an effective data augmentation method, mixup (Zhang et al., 2021b) has recently been applied to instance augmentation for CSL (Kalantidis et al., 2020; Kim et al., 2020; Shen et al., 2020; Lee et al., 2021). Among these methods, (Kalantidis et al., 2020) uses feature mixup for generating hard negative pairs. However, all these methods focus on unsupervised pre-training and cannot accurately generate hard pairs regarding classes. Comparatively, Core-tuning focuses on the fine-tuning of contrastive self-supervised models and can generate accurate hard positive/negative pairs for each class. Note that the hard pair generation strategy in Core-tuning is different from manifold mixup (Verma et al., 2019), which cannot be directly used to generate hard pairs.

Pre-training and Fine-tuning. In deep learning, it is a popular scheme to first pre-train a deep neural network on a large database (*e.g.*, ImageNet) and then fine-tune it on downstream tasks (Li et al., 2018; 2020). Supervised learning is the mainstream method for pre-training (Kornblith et al., 2019), whereas self-supervised learning is attracting increasing attention since it does not rely on rich annotations (Chen et al., 2020a;b). Most existing methods for fine-tuning, like L2-SP (Li et al., 2018) and DELTA (Li et al., 2019), are devised for supervised pre-trained models and tend to enforce some regularizer to prevent the fine-tuned models changing too much from the pre-trained ones. However, they may be unsuitable for contrastive self-supervised models, since downstream tasks are often different from the contrastive pre-training task, which may lead to negative transfer (Chen et al., 2019). Very recently, contrastive losses are used to fine-tune models (Günel et al., 2021; Zhong et al., 2021). However, these studies mainly add the contrastive loss to the objective of fine-tuning and cannot theoretically explain why it boosts fine-tuning. Meanwhile, they also ignore the two challenges in contrastive fine-tuning (see Figure 2), leading to inadequate fine-tuning performance.

3. Effects of Contrastive Loss

This section analyzes the benefits of the contrastive loss during fine-tuning, which will motivate our new method. Before that, we first define the problem and notations.

Problem Definition and Notation. This paper studies the fine-tuning of contrastive self-supervised visual models, which are pre-trained on a large-scale unlabeled database. During fine-tuning, let $\{(x_i, y_i)\}_{i=1}^n$ denote the target task dataset with n samples, where x_i is an instance with the one-hot label $y_i \in \mathbb{R}^K$ and K denotes the number of classes. We use a neural network model G to perform classification, which consists of a pre-trained feature encoder G_e and a new classifier G_y specific to the target task. Based on the network, we denote the learned features by $z_i = G_e(x_i)$ and the prediction by $\hat{y}_i = G_y(z_i)$. The model is generally fine-tuned with the cross-entropy loss.

Following (Boudiaf et al., 2020), we define the random variables of samples and labels as X and Y , and those of embeddings and predictions as $Z|X \sim G_e(X)$ and $\hat{Y}|Z \sim G_y(Z)$, respectively. Moreover, let p_Y be the distribution of Y , $p_{(Y,Z)}$ be the joint distribution of Y and Z , and $p_{Y|Z}$ be the conditional distribution of Y given Z . We define the entropy of Y as $\mathcal{H}(Y) := \mathbb{E}_{p_Y}[-\log p_Y(Y)]$ and the conditional entropy of Y given Z as $\mathcal{H}(Y|Z) := \mathbb{E}_{p_{(Y,Z)}}[-\log p_{Y|Z}(Y|Z)]$. Besides, we define the cross-entropy (CE) between Y and \hat{Y} by $\mathcal{H}(Y; \hat{Y}) := \mathbb{E}_{p_Y}[-\log p_{\hat{Y}}(Y)]$ and the conditional CE given Z by $\mathcal{H}(Y; \hat{Y}|Z) := \mathbb{E}_{p_{(Y,Z)}}[-\log p_{\hat{Y}|Z}(Y|Z)]$. Before our analysis, we first revisit the contrastive loss.

Contrastive loss. We use the supervised contrastive loss (Khosla et al., 2020) for fine-tuning, which is a variant of InfoNCE (Oord et al., 2018). Specifically, given a sample feature z_i as anchor, the contrastive loss takes the features from the same class to the anchor as positive pairs and those from diverse classes as negative pairs. Assuming features are ℓ_2 -normalized, the contrastive loss is computed by:

$$\mathcal{L}_{con} = -\frac{1}{n|P_i|} \sum_{i=1}^n \sum_{z_j \in P_i} \log \frac{e^{(z_i^\top z_j / \tau)}}{\sum_{z_k \in A_i} e^{(z_i^\top z_k / \tau)}}, \quad (1)$$

where τ is a temperature factor, while P_i and A_i denote the positive pair set and the full pair set of the anchor z_i , respectively. We next analyze the contrastive loss and find it has two effects during fine-tuning as follows.

3.1. Regularization Effect of Contrastive Loss

We first show the contrastive loss has regularization effectiveness on representation learning based on Theorem 1.

Theorem 1 *Assuming the features are ℓ_2 -normalized and the classes are balanced with equal data number, minimizing the contrastive loss is equivalent to minimizing the class-conditional entropy $\mathcal{H}(Z|Y)$ and maximizing the feature entropy $\mathcal{H}(Z)$:*

$$\mathcal{L}_{con} \propto \mathcal{H}(Z|Y) - \mathcal{H}(Z)$$

Please see the supplementary for the proof. This Theorem shows that \mathcal{L}_{con} explicitly regularizes the representation learning. On one hand, minimizing \mathcal{L}_{con} will minimize $\mathcal{H}(Z|Y)$, which encourages to learn a low-entropy cluster for each class (*i.e.*, high intra-class compactness). On the other hand, minimizing \mathcal{L}_{con} will maximize $\mathcal{H}(Z)$ and tends to learn a high-entropy feature space (*i.e.*, large inter-class separation degree). Such an effect can provide an additional regularization effect on features during fine-tuning, and it can be observed by the feature visualization in Figure 1. Note that this analysis is different from the analysis of unsupervised contrastive learning (Wang & Isola, 2020), which is specific to the instance level rather than the class level.

3.2. Optimization Effect of Contrastive Loss

We then show the contrastive loss has optimization effectiveness on model training based on Theorem 2.

Theorem 2 *Assuming the features are ℓ_2 -normalized and the classes are balanced, the contrastive loss is positive proportional to the infimum of conditional cross-entropy $\mathcal{H}(Y; \hat{Y}|Z)$, where the infimum is taken over classifiers:*

$$\mathcal{L}_{con} \propto \underbrace{\inf \mathcal{H}(Y; \hat{Y}|Z)}_{\text{Conditional CE}} - \mathcal{H}(Y)$$

Please see the supplementary for the proof. This theorem shows that \mathcal{L}_{con} boosts the model optimization. Concretely, the label Y is given by datasets, so its entropy $\mathcal{H}(Y)$ is a constant and can be ignored. Hence, minimizing \mathcal{L}_{con} will minimize the infimum of conditional cross-entropy $\mathcal{H}(Y; \hat{Y}|Z)$, which can provide an additional optimization effect as compared to the fine-tuning with only cross-entropy.

4. Contrast-Regularized Tuning

4.1. Overall Scheme

Motivated by the above analysis, we propose a new contrast-regularized tuning (Core-tuning) method¹ for better fine-tuning contrastive self-supervised models. Rather than simply adding the contrastive loss to the objective, Core-tuning further addresses two challenges in contrastive fine-tuning. First, hard sample pairs are informative for contrastive learning but the majority of training samples are easy to contrast (Wu et al., 2017), so it is important to mine hard pairs for more effective fine-tuning. Second, the classifier trained with cross-entropy is often sharp and may generalize poorly to the test data that is slightly different from the training data (Verma et al., 2019). Hence, it is important to explore how to improve the generalizability of the model.

To handle these challenges, Core-tuning applies two novel designs. First, Core-tuning generates both hard positive and hard negative pairs for more effective contrastive fine-tuning via a simple yet effective feature mixup strategy (see Section 4.2). Meanwhile, Core-tuning assigns higher importance weights to hard positive samples via a new focal contrastive loss \mathcal{L}_{con}^f (see Section 4.3). Second, Core-tuning further uses the mixed features for classifier training *w.r.t.* cross-entropy \mathcal{L}_{ce}^m , so that the learned decision boundary is smoother (see Section 4.4). The overall training procedure of Core-tuning is to minimize the following objective:

$$\min \underbrace{\mathcal{L}_{ce}^m}_{\text{cross-entropy loss}} + \underbrace{\eta \mathcal{L}_{con}^f}_{\text{focal contrastive loss}},$$

where η is a hyper-parameter to balance two losses.

¹Pseudo-code of Core-tuning is provided in the supplementary.

4.2. Hard Sample Pair Generation

As shown in Figure 2 (b-c), given features and labels $\{(z_i, y_i)\}_i^n$, we generate hard positive and hard negative pairs via a new feature mixup strategy, termed mixup-hard.

Mixing hard positive pairs. Given a feature anchor z_i , we first find out its hardest positive data z_i^{hp} and hardest negative data z_i^{hn} based on the cosine similarity. That is, z_i^{hp} is the positive data with the lowest cosine similarity to the anchor and z_i^{hn} is the negative data most similar to the anchor. We then generate the hard positive pair as a convex combination of z_i^{hp} and z_i^{hn} :

$$z_i^+ = \lambda z_i^{hp} + (1 - \lambda) z_i^{hn},$$

where $\lambda \sim \text{Beta}(\alpha, \alpha) \in [0, 1]$ (Zhang et al., 2018), and $\alpha \in (0, \infty)$ is a hyper-parameter to decide the distribution $\text{Beta}(\alpha, \alpha)$. To make the generated positive closer to positive pairs, we clip λ by $\lambda \geq \lambda_p$, where λ_p is a threshold and we set it to 0.8 by default. The generated pair is located between positives and negatives and thus is harder to contrast. We denote the generated hard positive set by $\mathcal{B}^+ = \{z_i^+\}_{i=1}^n$.

Mixing hard negative pairs. Given a feature anchor z_i , we randomly select a negative sample (z_i^n, y_i^n) to synthesize the hard negative pair and its corresponding soft label:

$$z_i^- = (1 - \lambda) z_i + \lambda z_i^n; \quad y_i^- = (1 - \lambda) y_i + \lambda y_i^n.$$

We clip $\lambda \sim \text{Beta}(\alpha, \alpha)$ by $\lambda \geq \lambda_n$ to make the generated negative closer to negative pairs, where λ_n is a threshold and also set to 0.8. The reason why we select a random negative sample instead of the hardest negative is that generating too hard negatives may result in false negatives and degrade performance. Note that semi-hard negatives may even yield better performance in metric learning (Wu et al., 2021). We denote the generated hard negative set by $\mathcal{B}^- = \{(z_i^-, y_i^-)\}_{i=1}^n$.

4.3. Hard Positive Reweighting

Since a nonlinear projection improves contrastive learning (Chen et al., 2020b,c), we first use a two-layer MLP head G_c to obtain ℓ_2 -normalized contrastive features $v_i = G_c(z_i) / \|G_c(z_i)\|_2$. Based on these features, one may directly use \mathcal{L}_{con} in Eq. (1) for fine-tuning. However, since hard positives are more informative for contrastive learning, we propose to assign higher importance weights to them. Inspired by the focal loss (Lin et al., 2017), we find the hard positive pairs generally lead to a low prediction probability $p_{ij} = \frac{\exp(v_i^\top v_j / \tau)}{\sum_{v_k \in A_i} \exp(v_i^\top v_k / \tau)}$. Thus, we reweight \mathcal{L}_{con} with $(1 - p_{ij})$ and develop a focal contrastive loss:

$$\mathcal{L}_{con}^f = - \frac{1}{n|P_i|} \sum_{i=1}^n \sum_{v_j \in P_i} (1 - p_{ij}) \log \frac{e^{(v_i^\top v_j / \tau)}}{\sum_{v_k \in A_i} e^{(v_i^\top v_k / \tau)}},$$

where P_i and A_i denote the anchor's positive pair set and full pair set, both of which contain the generated hard pairs.

Table 1. Comparisons of diverse methods for MoCo-v2 pre-trained ResNet-50 model fine-tuning on image classification in terms of top-1 accuracy. SL-CE-tuning denotes supervised pre-training on ImageNet and then fine-tuning with cross-entropy.

Method	ImageNet-20	CIFAR10	CIFAR100	Caltech101	DTD	Aircraft	Cars	Pets	Flowers	Avg.
SL-CE-tuning	91.01	94.23	83.40	93.39	74.40	87.03	89.77	92.17	98.78	89.35
CE-tuning	88.28	94.70	80.27	91.87	71.68	86.87	88.61	89.05	98.49	87.76
L2SP (Li et al., 2018)	88.49	95.14	81.43	91.98	72.18	86.55	89.00	89.43	98.66	88.10
M&M (Zhan et al., 2018)	88.53	95.02	80.58	92.91	72.43	87.45	88.90	89.60	98.57	88.22
DELTA (Li et al., 2019)	88.35	94.76	80.39	92.19	72.23	87.05	88.73	89.54	98.65	87.99
BSS (Chen et al., 2019)	88.34	94.84	80.40	91.95	72.22	87.18	88.50	89.50	98.57	87.94
RIFLE (Li et al., 2020)	89.06	94.71	80.36	91.94	72.45	87.60	89.72	90.05	98.70	88.29
SCL (Gunel et al., 2021)	89.29	95.33	81.49	92.84	72.73	87.44	89.37	89.71	98.65	88.54
Bi-tuning (Zhong et al., 2021)	89.06	95.12	81.42	92.83	73.53	87.39	89.41	89.90	98.57	88.58
Core-tuning (ours)	92.59	97.31	84.13	93.46	75.37	89.48	90.17	92.36	99.18	90.45

4.4. Smooth Classifier Learning

No matter whether the feature space is discriminative, the classifier trained with cross-entropy is often sharp and close to data, which leads to limited generalization performance (Verma et al., 2019). To address this, inspired by the effectiveness of mixup for helping learn a smoother decision boundary (Verma et al., 2019), we further use the mixed data from the hard negative set \mathcal{B}^- for classifier training:

$$\mathcal{L}_{ce}^m = -\frac{1}{n} \sum_{i=1}^n y_i \log(\hat{y}_i) - \frac{1}{|\mathcal{B}^-|} \sum_{(z_j, y_j) \in \mathcal{B}^-} y_j \log(G_y(z_j)),$$

One may also consider using the hard positive set \mathcal{B}^+ . Nevertheless, the mixed positives are located in the borderline area between positives and negatives, which has already been covered by the mixed negatives. Further using \mathcal{B}^+ will not bring extra performance improvement.

5. Experiments

We first test the effectiveness of Core-tuning on image classification and then apply it to image segmentation. Next, since Core-tuning potentially improves model generalizability, we further study how it affects model generalization to new domains and model robustness to adversarial samples.

5.1. Results on Image Classification

Settings. As there is no fine-tuning method devoted to contrastive self-supervised models, we compare Core-tuning with advanced fine-tuning methods for general models (e.g., supervised pre-trained models): L2SP (Li et al., 2018), M&M (Zhan et al., 2018), DELTA (Li et al., 2019), BSS (Chen et al., 2019), RIFLE (Li et al., 2020), SCL (Gunel et al., 2021) and Bi-tuning (Zhong et al., 2021). We denote the fine-tuning with cross-entropy by CE-tuning.

Following (Kornblith et al., 2019), we test on 9 image datasets, i.e., ImageNet-20, CIFAR10, CIFAR100, Caltech101, DTD, FGVC Aircraft, Standard Cars, Oxford-IIIT Pets and Oxford Flowers. Here, ImageNet-20 is an ImageNet subset with 20 classes, by combining the ImageNette and

ImageWoof datasets (Howard, 2020). These datasets cover a wide range of fine/coarse-grained object recognition tasks.

We implement Core-tuning in PyTorch, where the source codes will be available. Following (Ericsson et al., 2020), we use ResNet-50 ($1\times$), pre-trained by diverse CSL methods on ImageNet, as the network backbone. All checkpoints of pre-trained models are provided by authors or by the PyContrast repository². Following (Chen et al., 2020a), we perform parameter tuning for each dataset and select the best ones on a validation set. Both η and α are selected from $\{0.1, 1, 10\}$. Moreover, we set thresholds $\lambda_p = \lambda_n = 0.8$ and temperature $\tau = 0.07$ by default. All results are averaged over 3 runs in terms of the top-1 accuracy. More details of datasets and implementation are in our supplementary.

Comparisons with previous methods. We report the fine-tuning performance of the MoCo-v2 pre-trained model in Table 1. When using the standard CE-tuning, the MoCo-v2 pre-trained model performs worse than the supervised pre-trained model. This is because the self-supervised pre-trained model is less class-discriminative than the supervised pre-trained model due to the lack of annotations during pre-training. Moreover, the classic fine-tuning methods designed for supervised pre-trained models (e.g., L2SP and DELTA) cannot fine-tune the contrastive self-supervised model very well. One reason is that the contrastive pre-training task is essentially different from the downstream classification task, so strictly regularizing the difference between the contrastive self-supervised model and the fine-tuned model may lead to negative/poor transfer.

In addition, M&M, SCL and Bi-tuning use the triplet loss or the contrastive loss during fine-tuning. However, they ignore the two challenges in contrastive fine-tuning as mentioned in Figure 2, leading to limited model performance on downstream tasks. In contrast, Core-tuning handles those challenges well and improves the fine-tuning performance of contrastive self-supervised models a lot. This result demonstrates the superiority of Core-tuning. More results with the standard error are put in the supplementary.

²<https://github.com/HobbitLong/PyContrast>.

Table 2. Ablation studies of Core-tuning (Row 5) for fine-tuning MoCo-v2 pre-trained ResNet-50 on 9 natural image datasets in terms of top-1 accuracy. Here, \mathcal{L}_{con} is the original contrastive loss, while \mathcal{L}_{con}^f is our focal contrastive loss. Moreover, “mixup” denotes the manifold mixup, while “mixup-hard” indicates the proposed feature mixup strategy in our method.

\mathcal{L}_{ce}	\mathcal{L}_{con}	\mathcal{L}_{con}^f	mixup	mixup-hard	ImageNet-20	CIFAR10	CIFAR100	Caltech101	DTD	Aircraft	Cars	Pets	Flowers	Avg.
✓					88.28	94.70	80.27	91.87	71.68	86.87	88.61	89.05	98.49	87.76
✓	✓				89.29	95.33	81.49	92.84	72.73	87.44	89.37	89.71	98.65	88.54
✓			✓		90.67	95.43	81.03	92.68	73.31	88.37	89.06	91.37	98.74	88.96
✓	✓			✓	92.20	97.01	83.89	93.22	74.78	88.88	89.79	91.95	98.94	90.07
✓		✓		✓	92.59	97.31	84.13	93.46	75.37	89.48	90.17	92.36	99.18	90.45

Table 3. Fine-tuning performance of ResNet-50, pre-trained by diverse CSL methods. CE indicates cross-entropy.

Pre-training	Caltech101		DTD		Pets	
	CE	ours	CE	ours	CE	ours
InsDis	82.30	88.60	69.81	70.94	87.57	89.59
PIRL	84.23	89.29	68.95	71.72	86.87	89.52
MoCo-v2	91.87	93.46	71.68	75.37	89.05	92.36
SimCLR-v2	92.44	93.37	71.63	74.75	88.28	90.64
InfoMin	92.73	94.01	72.59	74.89	90.00	92.34

Table 4. Fine-tuning performance of diverse network architectures, pre-trained by InfoMin. CE indicates cross-entropy.

Architecture	Caltech101		DTD		Pets	
	CE	ours	CE	ours	CE	ours
ResNet-50	92.73	94.01	72.59	74.89	90.00	92.34
ResNet-101	93.06	94.33	73.38	75.09	90.84	92.91
ResNet-152	93.39	94.66	73.74	75.42	91.08	92.97
ResNext-101	93.71	95.12	74.43	75.97	91.97	94.04
ResNext-152	93.92	95.19	74.76	76.22	92.70	94.49

Ablation studies of Core-tuning. We conduct ablation studies for Core-tuning regarding the focal contrastive loss and the mixup-hard strategy. As shown in Table 2, each component improves the performance. Note that the mixup in Row 3 is the manifold mixup (Verma et al., 2019), which is essentially designed for classification and is expected to outperform our mixup-hard strategy regarding classification performance. However, our proposed Core-tuning (Row 5) still shows obvious improvement on all datasets, which strongly verifies the value of contrastive fine-tuning.

Results on different CSL methods. In previous experiments, we fine-tune the ResNet-50 model pre-trained by MoCo-v2, but it is unclear whether Core-tuning can be applied to fine-tune models pre-trained by other CSL methods. Hence, we further use Core-tuning to fine-tune ResNet-50, pre-trained by InsDis (Wu et al., 2018), PIRL (Misra & Maaten, 2020), SimCLR-v2 (Chen et al., 2020b) and InfoMin (Tian et al., 2020). As shown in Table 3, Core-tuning fine-tunes all pre-trained models consistently better than CE-tuning on 3 image classification datasets.

Results on different network architectures. Previous experiments are based on ResNet-50, while it is unclear whether Core-tuning can be applied to fine-tune other network architectures. Hence, we further apply Core-tuning to fine-tune diverse architectures, i.e., ResNet-101, ResNet-152, ResNext-101 and ResNext-152 (Xie et al., 2017). All

Table 5. Fine-tuning performance of the MoCo-v2 pre-trained ResNet-50 with diverse numbers of labeled data.

Method	Sampling Rates on ImageNet-20			
	10%	25%	50%	75%
CE-tuning	52.97+/-3.96	63.17+/-3.94	81.78+/-1.37	85.85+/-0.11
Bi-tuning	60.50+/-1.11	75.86+/-0.74	83.18+/-0.27	87.19+/-0.19
Core-tuning	78.64+/-0.58	84.48+/-0.34	89.09+/-0.40	90.93+/-0.24

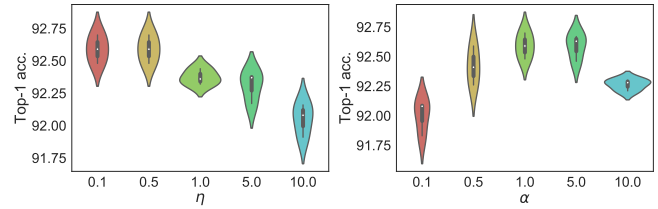


Figure 3. Sensitivity analysis of η and α in Core-tuning on ImageNet-20 based on MoCo-v2 pre-trained ResNet-50. Each run tests one factor and fixes others. Best viewed in color.

these networks are pre-trained by InfoMin (Tian et al., 2020). As shown in Table 4, Core-tuning fine-tunes all network architectures well on 3 image classification datasets.

Results on different data sizes. The labeled data may be scarce in downstream tasks. Hence, we further evaluate Core-tuning on Imagenet-20 with different sampling rates of data. We report the results in Table 5, while the results on the full ImageNet-20 have been listed in Table 1. Specifically, Core-tuning outperforms baselines in all cases. Note that when the data is very scarce (e.g., 10%), the fine-tuning performance of CE-tuning degrades and fluctuates significantly, in which case Core-tuning obtains more significant improvement and achieves more stable performance.

Parameter sensitivity. We next analyze the parameter sensitivity in Core-tuning. We first discuss the influence of the loss trade-off parameter η and the mixup sampling factor α based on ImageNet-20. Each run tests one parameter and fixes others. As shown in Figure 3, when $\eta=0.5$ and $\alpha=5$, Core-tuning performs slightly better on ImageNet-20. Note that the best η and α can be different on diverse datasets.

We then analyze the negative/positive pair thresholds (λ_n, λ_p) in the devised mixup-hard strategy. The results on ImageNet-20 are reported in Table 6. On the one hand, λ_n satisfies our expectation that the generated hard negative pairs should be closer to negatives, i.e., a larger λ_n can lead to better performance. On the other hand, we find when no

Table 6. Threshold analysis for hard pair generation in Core-tuning on ImageNet-20 based on MoCo-v2 pre-trained ResNet-50. Each run tests one parameter and fixes others.

Thresholds	0	0.2	0.4	0.6	0.8
Negative pair threshold λ_n	91.55	91.94	92.19	92.36	92.59
Positive pair threshold λ_p	92.73	92.68	92.64	92.60	92.59

crop is conducted for hard positive generation (*i.e.*, $\lambda_p=0$), the performance is slightly better. We conjecture that since the generated hard positives are located in the borderline area between positives and negatives, allowing the generated hard positives to close to negatives may have a margin effect on contrastive learning and thus boosts performance. Despite this, Core-tuning with a large λ_p , like 0.8, also performs similarly well. Due to the page limitation, we put more results of parameter sensitivity in the supplementary.

5.2. Results on Semantic Segmentation

We next apply Core-tuning to fine-tune contrastive self-supervised models on semantic segmentation.

Implementation details. We adopt the DeepLab-V3 framework (Chen et al., 2017) for PASCAL VOC semantic segmentation and use the contrastive pre-trained ResNet-50 model as the backbone. In Core-tuning, we enforce the contrastive regularizer after the penultimate layer of ResNet-50 via an additional global average pooling. Due to the characteristics of dense prediction, we only generate hard positive pairs and do not use the mixed data for classifier training. Following (Wang et al., 2020), the model is fine-tuned on VOC train_aug2012 set for 30k steps via stochastic gradient descent and evaluated on val2012 set. The image is rescaled to 513×513 with random crop and flips for training and with center crop for evaluation. The batch size and the output stride are 16. Besides, we set the initial learning rate to 0.1 and adjust it via the poly learning rate schedule. The momentum parameter is set to 0.9, and the factor of weight decay is set to 10^{-4} . Other parameters are the same as image classification. We use three metrics: Mean Pixel Accuracy (MPA), Frequency Weighted Intersection over Union (FWIoU) and Mean Intersection over Union (MIoU).

Results. We report the results in Table 7, in which Core-tuning contributes to the fine-tuning performance of all contrastive pre-trained models in terms of MPA, FWIoU and MIoU. Such a promising result demonstrate the effectiveness of Core-tuning on semantic segmentation. Interestingly, we find that with standard fine-tuning, the models pre-trained by MoCo-v2, SimCLR-v2 and InfoMin have already outperformed the supervised pre-trained model. One explanation is that contrastive self-supervised pre-training may keep more visual information, compared to supervised pre-training that mainly extracts information specific to classification (Zhao et al., 2021). In other words, unsupervised

Table 7. Fine-tuning performance on PASCAL VOC semantic segmentation based on DeepLab-V3 with ResNet-50, pre-trained by diverse CSL methods. CE indicates cross-entropy.

Pre-training	Fine-tuning	MPA	FWIoU	MIoU
Supervised	CE	87.10+/-0.20	89.12+/-0.17	76.52+/-0.34
InsDis	CE	83.64+/-0.12	88.23+/-0.08	74.14+/-0.21
	ours	84.53+/-0.31	88.67+/-0.07	74.81+/-0.13
PIRL	CE	83.16+/-0.26	88.22+/-0.24	73.99+/-0.42
	ours	85.30+/-0.24	88.95+/-0.08	75.49+/-0.36
MoCo-v2	CE	87.31+/-0.31	90.26+/-0.12	78.42+/-0.28
	ours	88.76+/-0.34	90.75+/-0.04	79.62+/-0.12
SimCLR-v2	CE	87.37+/-0.48	90.27+/-0.12	78.16+/-0.19
	ours	87.95+/-0.20	90.71+/-0.13	79.15+/-0.33
InfoMin	CE	87.17+/-0.20	89.84+/-0.09	77.84+/-0.24
	ours	88.92+/-0.36	90.65+/-0.09	79.48+/-0.30

contrastive learning may extract more beneficial information for dense prediction, which inspires us to explore unsupervised contrastive regularizers in the future.

5.3. Effectiveness on Cross-domain Generalization

The generalizability of deep networks to unseen domains is important for their application to real-world scenarios (Dou et al., 2019). We thus wonder whether Core-tuning also benefits model generalization. Therefore, we apply Core-tuning to the task of domain generalization (DG).

Implementation details. The task of DG aims to train a model on multiple source domains and expect it to generalize well to an unseen target domain. Specifically, we use MoCo-v2 pre-trained ResNet-50 as the backbone, and evaluate Core-tuning on 3 benchmark datasets, *i.e.*, PACS (Li et al., 2017), VLCS (Fang et al., 2013) and Office-Home (Venkateswara et al., 2017). In the training process, we use Adam optimizer with the batch size 32. The learning rate is set to 5×10^{-5} and the training step is 20,000. More implementation details are put in the supplementary.

Results. We report results in Table 8 and draw several observations as follows. First, when fine-tuning with cross-entropy, the contrastive self-supervised model performs worse than the supervised pre-trained model. This results from the relatively worse discriminative abilities of the contrastive self-supervised model, which can also be found in Table 1. Second, enforcing contrastive regularizer during fine-tuning improves DG performance, since the contrastive regularizer helps learn more discriminative features (refer to Theorem 1) and also helps alleviate distribution shifts among domains (Kang et al., 2019), hence leading to better performance. Last, Core-tuning further improves the generalization performance of models on all datasets. This is because hard pair generation further boosts contrastive learning, while smooth classifier learning also benefits model generalizability. We thus conclude that Core-tuning is beneficial to model generalization.

Table 8. Domain generalization accuracies of diverse fine-tuning methods for MoCo-v2 pre-trained ResNet-50. CE means cross-entropy; CE-Con enhances CE with the contrastive loss.

Pre-training	Fine-tuning	PACS				
		A	C	P	S	Avg.
Supervised	CE	83.65	79.21	96.11	81.46	85.11
MoCo-v2	CE	78.71	76.92	90.87	75.67	80.54
	CE-Con	85.11	81.77	95.58	80.12	85.65
	ours	87.31	84.06	97.53	83.43	88.08
Pre-training	Fine-tuning	VLCS				
		C	L	V	S	Avg.
Supervised	CE	98.41	63.81	68.55	75.45	76.56
MoCo-v2	CE	94.96	66.87	68.96	64.98	73.94
	CE-Con	95.94	67.76	69.31	73.57	77.67
	ours	98.50	68.19	73.15	81.53	80.34
Pre-training	Fine-tuning	Office-Home				
		A	C	P	R	Avg.
Supervised	CE	56.08	50.83	72.49	75.21	63.82
MoCo-v2	CE	50.31	48.91	64.72	68.76	58.18
	CE-Con	55.87	50.23	71.51	74.99	63.15
	ours	58.70	52.43	72.89	75.36	64.85

5.4. Robustness to Adversarial Samples

As is known, deep networks are fragile to adversarial attack (Szegedy et al., 2014). We thus wonder whether Core-tuning also benefits model robustness to adversarial samples in the setting of adversarial training (AT).

Implementation details. We use MoCo-v2 pre-trained ResNet-50 as the network backbone, and use the Projected Gradient Descent (PGD) (Madry et al., 2018) to generate adversarial samples with ℓ_2 attack (strength $\sigma=0.5$) and ℓ_∞ attack (strength $\sigma=4/255$). During AT, we use both original samples and adversarial samples for fine-tuning. Moreover, we use the clean accuracy on original samples and the robust accuracy on adversarial samples as metrics. More implementation details are put in the supplementary.

Results. We draw several observations based on the results on 3 image datasets in Table 9 and the results on CIFAR10 in the supplementary. First, despite good clean accuracy, standard fine-tuning with cross-entropy cannot defend against adversarial attack, leading to poor robust accuracy. Second, AT with cross-entropy improves the robust accuracy significantly, but it inevitably degrades the clean accuracy due to the accuracy-robustness trade-off (Tsipras et al., 2019). In contrast, the contrastive regularizer improves both robust and clean accuracies. This is because contrastive learning helps improve robustness generalization (*i.e.*, alleviating the distribution shifts between clean samples and adversarial samples), thus leading to better performance.

Last, Core-tuning further boosts AT and, surprisingly, even achieves better clean accuracy than the standard fine-tuning under the ℓ_2 attack. To our knowledge, this is quite promising since even the most advanced AT methods (Zhang et al.,

Table 9. Adversarial training performance of MoCo-v2 pre-trained ResNet-50 under the attack of PGD-10 in terms of robust and clean accuracies. CE indicates cross-entropy; AT-CE indicates adversarial training (AT) with CE; AT-CE-Con enhances AT-CE with the contrastive loss; AT-ours uses Core-tuning for AT.

Method	PGD - ℓ_2 attack ($\epsilon = 0.5$)					
	Caltech101		DTD		Pets	
	Robust	Clean	Robust	Clean	Robust	Clean
CE	55.69	91.87	42.25	71.68	30.94	89.05
AT-CE	87.35	91.61	61.93	68.81	78.67	86.25
AT-CE-Con	88.67	92.61	64.75	71.24	79.53	87.01
AT-ours	89.21	92.83	66.49	72.94	82.54	89.22
Method	PGD - ℓ_∞ attack ($\epsilon = 4/255$)					
	Caltech101		DTD		Pets	
	Robust	Clean	Robust	Clean	Robust	Clean
CE	27.03	91.87	18.37	71.68	4.63	89.05
AT-CE	78.61	90.65	47.27	67.13	63.59	84.21
AT-CE-Con	79.87	91.08	48.95	69.07	65.60	86.85
AT-ours	80.73	91.64	49.43	70.65	67.98	87.20

2021a; Yang et al., 2020) find it difficult to conquer the accuracy-robustness trade-off (Zhang et al., 2019). The improvement is mainly derived from that both contrastive learning and smooth classifier learning boost the robustness generalization. We thus conclude that Core-tuning is beneficial to model robustness. We also hope that Core-tuning can motivate people to rethink the accuracy-robustness trade-off in adversarial training in the future.

6. Conclusions

This paper studied how to fine-tune contrastive self-supervised visual models. We theoretically show that optimizing the contrastive loss during fine-tuning has regularization effectiveness on representation learning as well as optimization effectiveness on classifier training, both of which benefit model fine-tuning. We thus proposed a novel contrast-regularized tuning (Core-tuning) method to fine-tune contrastive self-supervised visual models. We empirically evaluated Core-tuning on both image classification and semantic segmentation tasks. Promising results verify the effectiveness of the proposed method. Also, we empirically found that Core-tuning is beneficial to model generalization and robustness on downstream tasks. We thus recommend using Core-tuning as a standard baseline to fine-tune contrastive self-supervised visual models.

Future directions. We first call for more attention to the fine-tuning of contrastive self-supervised visual models on understanding its underlying theories and better approaches. Moreover, in the future, we will explore how to extend the proposed Core-tuning to fine-tune supervised pre-trained models and language models on different downstream tasks. We are also interested in exploring unsupervised contrastive regularizers for fine-tuning in the future.

References

- Boudiaf, M., Rony, J., et al. A unifying mutual information view of metric learning: cross-entropy vs. pairwise losses. In *European Conference on Computer Vision*, 2020.
- Chen, L.-C., Papandreou, G., Schroff, F., and Adam, H. Rethinking atrous convolution for semantic image segmentation. *ArXiv*, 2017.
- Chen, T., Kornblith, S., Norouzi, M., and Hinton, G. A simple framework for contrastive learning of visual representations. In *International Conference on Machine Learning*, 2020a.
- Chen, T., Kornblith, S., Swersky, K., Norouzi, M., and Hinton, G. Big self-supervised models are strong semi-supervised learners. In *Advances in Neural Information Processing Systems*, 2020b.
- Chen, X., Wang, S., et al. Catastrophic forgetting meets negative transfer: Batch spectral shrinkage for safe transfer learning. In *Advances in Neural Information Processing Systems*, 2019.
- Chen, X., Fan, H., Girshick, R., and He, K. Improved baselines with momentum contrastive learning. *ArXiv*, 2020c.
- Dou, Q., Castro, D. C., Kamnitsas, K., and Glocker, B. Domain generalization via model-agnostic learning of semantic features. In *Advances in Neural Information Processing Systems*, 2019.
- Ericsson, L., Gouk, H., and Hospedales, T. M. How well do self-supervised models transfer? *ArXiv*, 2020.
- Fang, C., Xu, Y., et al. Unbiased metric learning: On the utilization of multiple datasets and web images for softening bias. In *International Conference on Computer Vision*, 2013.
- Gidaris, S., Singh, P., and Komodakis, N. Unsupervised representation learning by predicting image rotations. In *International Conference on Learning Representations*, 2018.
- Gunel, B., Du, J., Conneau, A., and Stoyanov, V. Supervised contrastive learning for pre-trained language model fine-tuning. In *International Conference on Learning Representations*, 2021.
- Harwood, B., Kumar BG, V., Carneiro, G., Reid, I., and Drummond, T. Smart mining for deep metric learning. In *International Conference on Computer Vision*, pp. 2821–2829, 2017.
- He, K., Fan, H., Wu, Y., Xie, S., and Girshick, R. Momentum contrast for unsupervised visual representation learning. In *Computer Vision and Pattern Recognition*, 2020.
- Howard, J. The imagenette and imagewoof datasets, 2020. URL <https://github.com/fastai/imagenette/>.
- Kalantidis, Y., Sariyildiz, M. B., Pion, N., Weinzaepfel, P., and Larlus, D. Hard negative mixing for contrastive learning. In *Advances in Neural Information Processing Systems*, 2020.
- Kang, G., Jiang, L., Yang, Y., and Hauptmann, A. G. Contrastive adaptation network for unsupervised domain adaptation. In *Computer Vision and Pattern Recognition*, 2019.
- Khosla, P., Teterwak, P., et al. Supervised contrastive learning. In *Advances in Neural Information Processing Systems*, 2020.
- Kim, S., Lee, G., Bae, S., and Yun, S.-Y. Mixco: Mix-up contrastive learning for visual representation. *ArXiv*, 2020.
- Kornblith, S., Shlens, J., and Le, Q. V. Do better imagenet models transfer better? In *Computer Vision and Pattern Recognition*, pp. 2661–2671, 2019.
- Larsson, G., Maire, M., and Shakhnarovich, G. Learning representations for automatic colorization. In *European Conference on Computer Vision*, pp. 577–593, 2016.
- Lee, K., Zhu, Y., Sohn, K., Li, C.-L., Shin, J., and Lee, H. i-mix: A strategy for regularizing contrastive representation learning. In *International Conference on Learning Representations*, 2021.
- Li, D., Yang, Y., Song, Y.-Z., and Hospedales, T. M. Deeper, broader and artier domain generalization. In *International Conference on Computer Vision*, pp. 5542–5550, 2017.
- Li, X., Grandvalet, Y., and Davoine, F. Explicit inductive bias for transfer learning with convolutional networks. In *International Conference on Machine Learning*, 2018.
- Li, X., Xiong, H., et al. Delta: Deep learning transfer using feature map with attention for convolutional networks. In *International Conference on Learning Representations*, 2019.
- Li, X., Xiong, H., et al. Rifle: Backpropagation in depth for deep transfer learning through re-initializing the fully-connected layer. In *International Conference on Machine Learning*, 2020.
- Lin, T.-Y., Goyal, P., Girshick, R., He, K., and Dollár, P. Focal loss for dense object detection. In *International Conference on Computer Vision*, pp. 2980–2988, 2017.
- Liu, W., Wen, Y., Yu, Z., and Yang, M. Large-margin softmax loss for convolutional neural networks. In *International Conference on Machine Learning*, pp. 507–516, 2016.
- Madry, A., Makelov, A., Schmidt, L., Tsipras, D., and Vladu, A. Towards deep learning models resistant to adversarial attacks. In *International Conference on Learning Representations*, 2018.
- Misra, I. and Maaten, L. v. d. Self-supervised learning of pretext-invariant representations. In *Computer Vision and Pattern Recognition*, pp. 6707–6717, 2020.
- Oord, A. v. d., Li, Y., and Vinyals, O. Representation learning with contrastive predictive coding. *ArXiv*, 2018.
- Shen, Z., Liu, Z., Liu, Z., Savvides, M., and Darrell, T. Rethinking image mixture for unsupervised visual representation learning. *ArXiv*, 2020.
- Szegedy, C., Zaremba, W., Sutskever, I., Bruna, J., Erhan, D., Goodfellow, I., and Fergus, R. Intriguing properties of neural networks. In *International Conference on Learning Representations*, 2014.
- Tian, Y., Sun, C., Poole, B., Krishnan, D., Schmid, C., and Isola, P. What makes for good views for contrastive learning. In *Advances in Neural Information Processing Systems*, 2020.
- Tsipras, D., Santurkar, S., Engstrom, L., Turner, A., and Madry, A. Robustness may be at odds with accuracy. In *International Conference on Learning Representations*, 2019.
- Venkateswara, H., Eusebio, J., Chakraborty, S., and Panchanathan, S. Deep hashing network for unsupervised domain adaptation. In *Computer Vision and Pattern Recognition*, 2017.

- Verma, V., Lamb, A., Beckham, C., Najafi, A., Mitliagkas, I., Lopez-Paz, D., and Bengio, Y. Manifold mixup: Better representations by interpolating hidden states. In *International Conference on Machine Learning*, pp. 6438–6447, 2019.
- Wang, T. and Isola, P. Understanding contrastive representation learning through alignment and uniformity on the hypersphere. In *International Conference on Machine Learning*, 2020.
- Wang, X., Zhang, R., Shen, C., Kong, T., and Li, L. Dense contrastive learning for self-supervised visual pre-training. *ArXiv*, 2020.
- Wen, Y., Zhang, K., Li, Z., and Qiao, Y. A discriminative feature learning approach for deep face recognition. In *European Conference on Computer Vision*, pp. 499–515, 2016.
- Wu, C.-Y., Manmatha, R., Smola, A. J., and Krahenbuhl, P. Sampling matters in deep embedding learning. In *International Conference on Computer Vision*, pp. 2840–2848, 2017.
- Wu, M., Mosse, M., Zhuang, C., Yamins, D., and Goodman, N. Conditional negative sampling for contrastive learning of visual representations. In *International Conference on Learning Representations*, 2021.
- Wu, Z., Xiong, Y., Yu, S. X., and Lin, D. Unsupervised feature learning via non-parametric instance discrimination. In *Computer Vision and Pattern Recognition*, 2018.
- Xie, S., Girshick, R., Dollár, P., Tu, Z., and He, K. Aggregated residual transformations for deep neural networks. In *Computer Vision and Pattern Recognition*, pp. 1492–1500, 2017.
- Yang, Y.-Y., Rashtchian, C., Zhang, H., Salakhutdinov, R., and Chaudhuri, K. A closer look at accuracy vs. robustness. In *Advances in Neural Information Processing Systems*, 2020.
- Zhan, X., Liu, Z., Luo, P., Tang, X., and Loy, C. C. Mix-and-match tuning for self-supervised semantic segmentation. In *AAAI Conference on Artificial Intelligence*, 2018.
- Zhang, H., Cisse, M., Dauphin, Y. N., and Lopez-Paz, D. mixup: Beyond empirical risk minimization. In *International Conference on Learning Representations*, 2018.
- Zhang, H., Yu, Y., Jiao, J., Xing, E., El Ghaoui, L., and Jordan, M. Theoretically principled trade-off between robustness and accuracy. In *International Conference on Machine Learning*, 2019.
- Zhang, J., Zhu, J., Niu, G., Han, B., Sugiyama, M., and Kankanhalli, M. Geometry-aware instance-reweighted adversarial training. In *International Conference on Learning Representations*, 2021a.
- Zhang, L., Deng, Z., Kawaguchi, K., Ghorbani, A., and Zou, J. How does mixup help with robustness and generalization? In *International Conference on Learning Representations*, 2021b.
- Zhao, N., Wu, Z., Lau, R. W., and Lin, S. What makes instance discrimination good for transfer learning? In *International Conference on Learning Representations*, 2021.
- Zhong, J., Wang, X., Kou, Z., Wang, J., and Long, M. Bi-tuning of pre-trained representations. *Submission to International Conference on Learning Representations*, 2021.

Supplementary Materials: Unleashing the Power of Contrastive Self-Supervised Visual Models via Contrast-Regularized Fine-Tuning

Yifan Zhang¹ Bryan Hooi¹ Dapeng Hu¹ Jian Liang¹ Jiashi Feng¹

Abstract

This supplementary material provides proofs for the analysis of the contrastive loss (See App. A), the pseudo-code of the proposed method (See App. B), more implementation details (See App. C), and more empirical results (See App. D) for our submission.

A. Proof of Theoretical Analysis

This appendix provides proofs for both Theorems 1 and 2.

A.1. Proof for Theorem 1

Theorem 1 Assuming the features are ℓ_2 -normalized and the classes are balanced with equal data number, minimizing the contrastive loss is equivalent to minimizing the class-conditional entropy $\mathcal{H}(Z|Y)$ and maximizing the feature entropy $\mathcal{H}(Z)$:

$$\mathcal{L}_{con} \propto \mathcal{H}(Z|Y) - \mathcal{H}(Z)$$

Proof Let \mathcal{Z}_k denote the sample set of the class k . We assume the classes of samples are balanced so that the sample number of each class is constant $|\mathcal{Z}_k| = \frac{n}{K}$, where n denotes the total number of samples and K indicates the number of classes. Let us start by splitting the contrastive loss into two terms.

$$\begin{aligned} \mathcal{L}_{con} &= -\frac{1}{n|P_i|} \sum_{i=1}^n \sum_{z_j \in P_i} \log \frac{e^{(v_i^\top v_j / \tau)}}{\sum_{v_k \in A_i} e^{(v_i^\top v_k / \tau)}} \\ &= -\frac{1}{n|P_i|} \sum_{i=1}^n \sum_{z_j \in P_i} \frac{z_i^\top z_j}{\tau} + \frac{1}{n} \sum_{i=1}^n \log \sum_{z_k \in A_i} e^{(\frac{z_i^\top z_j}{\tau})}. \end{aligned} \quad (1)$$

Let $c_k = \frac{1}{|\mathcal{Z}_k|} \sum_{z \in \mathcal{Z}_k} z$ denote the hard mean of all features from the class k , and let the symbol $\stackrel{c}{=}$ indicate equality up

¹National University of Singapore. Correspondence to: Yifan Zhang <yifan.zhang@u.nus.edu>, Jiashi Feng <elefja@nus.edu.sg>.

to a multiplicative and/or additive constant. We first analyze the first term in Eq. (1) by connecting it to a tightness term of the center loss, i.e., $\sum_{z_i \in \mathcal{Z}_k} \|z_i - c_k\|^2$ (Wen et al., 2016):

$$\begin{aligned} \sum_{z_i, z_j \in \mathcal{Z}_k} -\frac{z_i^\top z_j}{\tau} &\stackrel{c}{=} \frac{1}{|\mathcal{Z}_k|} \sum_{z_i, z_j \in \mathcal{Z}_k} -z_i^\top z_j \\ &\stackrel{c}{=} \frac{1}{|\mathcal{Z}_k|} \sum_{z_i, z_j \in \mathcal{Z}_k} \|z_i\|^2 - z_i^\top z_j \\ &= \sum_{z_i \in \mathcal{Z}_k} \|z_i\|^2 - \frac{1}{|\mathcal{Z}_k|} \sum_{z_i \in \mathcal{Z}_k} \sum_{z_j \in \mathcal{Z}_k} z_i^\top z_j \\ &= \sum_{z_i \in \mathcal{Z}_k} \|z_i\|^2 - 2 \frac{1}{|\mathcal{Z}_k|} \sum_{z_i \in \mathcal{Z}_k} \sum_{z_j \in \mathcal{Z}_k} z_i^\top z_j \\ &\quad + \frac{1}{|\mathcal{Z}_k|} \sum_{z_i \in \mathcal{Z}_k} \sum_{z_j \in \mathcal{Z}_k} z_i^\top z_j \\ &= \sum_{z_i \in \mathcal{Z}_k} \|z_i\|^2 - 2 z_i^\top c_k + \|c_k\|^2 \\ &= \sum_{z_i \in \mathcal{Z}_k} \|z_i - c_k\|^2, \end{aligned}$$

where we use the property of ℓ_2 -normalized features that $\|z_i\|^2 = \|z_j\|^2 = 1$ and the definition of the class hard mean $c_k = \frac{1}{|\mathcal{Z}_k|} \sum_{z \in \mathcal{Z}_k} z$.

By summing over all classes k , we obtain:

$$\sum_{i=1}^n \sum_{z_j \in P_i} -\frac{z_i^\top z_j}{\tau} \stackrel{c}{=} \sum_{i=1}^n \|z_i - c_{y_i}\|^2.$$

Based on this equation, following (Boudiaf et al., 2020), we can interpret the first term in Eq. (1) as a conditional cross-entropy between Z and another random variable \bar{Z} , whose conditional distribution given Y is a standard Gaussian centered around $c_Y: \bar{Z}|Y \sim \mathcal{N}(c_Y, I)$:

$$\begin{aligned} -\frac{1}{n|P_i|} \sum_{i=1}^n \sum_{z_j \in P_i} \frac{z_i^\top z_j}{\tau} &\stackrel{c}{=} \mathcal{H}(Z; \bar{Z}|Y) \\ &= \mathcal{H}(Z|Y) + \mathcal{D}_{KL}(Z||\bar{Z}|Y). \end{aligned}$$

Based on this, we know that the first term in Eq. (1) is an upper bound on the conditional entropy of features Z given

labels Y :

$$-\frac{1}{n|P_i|} \sum_{i=1}^n \sum_{z_j \in P_i} \frac{z_i^\top z_j}{\tau} \stackrel{c}{\geq} \mathcal{H}(Z|Y).$$

where the symbol $\stackrel{c}{\geq}$ indicates “larger than”, up to a multiplicative and/or a additive constant. When $Z|Y \sim \mathcal{N}(c_y, i)$, the bound is tight. As a result, minimizing the first term in Eq. (1) is equivalent to minimizing $\mathcal{H}(Z|Y)$:

$$-\frac{1}{n|P_i|} \sum_{i=1}^n \sum_{z_j \in P_i} \frac{z_i^\top z_j}{\tau} \propto \mathcal{H}(Z|Y). \quad (2)$$

This concludes the proof for the relationship of the first term in Eq. (1).

We then analyze the second term in Eq. (1), which has the following relationship:

$$\begin{aligned} & \frac{1}{n} \sum_{i=1}^n \log \sum_{z_k \in A_i} e^{\left(\frac{z_i^\top z_k}{\tau}\right)} \\ &= \frac{1}{n} \sum_{i=1}^n \log \left(\sum_{k:y_i=y_k} e^{\left(\frac{z_i^\top z_k}{\tau}\right)} + \sum_{k:y_i \neq y_k} e^{\left(\frac{z_i^\top z_k}{\tau}\right)} \right) \\ &\geq \frac{1}{n} \sum_{i=1}^n \log \left(\sum_{k:y_i \neq y_k} e^{\left(\frac{z_i^\top z_k}{\tau}\right)} \right) \\ &\stackrel{c}{\geq} \frac{1}{n} \sum_{i=1}^n \sum_{k:y_i \neq y_k} \frac{z_i^\top z_k}{\tau} \\ &= \frac{1}{n} \sum_{i=1}^n \sum_{k=1}^n \frac{z_i^\top z_k}{\tau} - \frac{1}{n} \sum_{i=1}^n \sum_{k:y_i=y_k} \frac{z_i^\top z_k}{\tau} \\ &\stackrel{c}{=} -\frac{1}{n} \sum_{i=1}^n \sum_{k=1}^n \|z_i - z_k\|^2 - \frac{1}{n} \sum_{i=1}^n \sum_{k:y_i=y_k} \frac{z_i^\top z_k}{\tau}, \quad (3) \end{aligned}$$

where we use Jensen’s inequality in the fourth line. The first term in Eq. (3) can be viewed as a differential entropy estimator of features Z provided by (Wang & Sha, 2011):

$$\begin{aligned} \hat{\mathcal{H}}(Z) &= \frac{d}{n(n-1)} \sum_{i=1}^n \sum_{k=1}^n \log \|z_i - z_k\|^2 \\ &= \frac{1}{n} \sum_{i=1}^n \sum_{k=1}^n \|z_i - z_k\|^2, \quad (4) \end{aligned}$$

where d is the dimension of features. Combining Eq. (3) and Eq. (4) leads to:

$$\frac{1}{n} \sum_{i=1}^n \log \sum_{z_k \in A_i} e^{\left(\frac{z_i^\top z_k}{\tau}\right)} \stackrel{c}{\geq} -\mathcal{H}(Z) - \frac{1}{n} \sum_{i=1}^n \sum_{k:y_i=y_k} \frac{z_i^\top z_k}{\tau}. \quad (5)$$

The second term in the right side of Eq. (5) is essentially a redundant term with the first term in Eq. (1), so we ignore it here. Then, we know that minimizing the second term in Eq. (1) is equivalent to maximizing $\mathcal{H}(Z)$:

$$\frac{1}{n} \sum_{i=1}^n \log \sum_{z_k \in A_i} e^{\left(\frac{z_i^\top z_k}{\tau}\right)} \propto -\mathcal{H}(Z). \quad (6)$$

Combining Eq. (2) and Eq. (6), we conclude the proof of Theorem 1. \square

A.2. Proof for Theorem 2

Theorem 2 Assuming the features are ℓ_2 -normalized and the classes are balanced, the contrastive loss is positive proportional to the infimum of conditional cross-entropy $\mathcal{H}(Y; \hat{Y}|Z)$, where the infimum is taken over classifiers:

$$\mathcal{L}_{con} \propto \inf_{\text{Conditional CE}} \mathcal{H}(Y; \hat{Y}|Z) - \mathcal{H}(Y)$$

Proof The mutual information between features Z and labels Y can be defined in two ways:

$$\mathcal{I}(Z; Y) = \mathcal{H}(Y) - \mathcal{H}(Y|Z) = \mathcal{H}(Z) - \mathcal{H}(Z|Y). \quad (7)$$

Based on Theorem 1, we know that:

$$\mathcal{L}_{con} \propto \mathcal{H}(Z|Y) - \mathcal{H}(Z) = -\mathcal{I}(Z; Y). \quad (8)$$

Combining Eq. (7) and Eq. (8), we have:

$$\mathcal{L}_{con} \propto \mathcal{H}(Y|Z) - \mathcal{H}(Y). \quad (9)$$

Then, we relate the conditional entropy $\mathcal{H}(Y|Z)$ to the cross entropy loss:

$$\mathcal{H}(Y; \hat{Y}|Z) = \mathcal{H}(Y|Z) + \mathcal{D}_{KL}(Y \parallel \hat{Y}|Z). \quad (10)$$

According to Eq. (10), when we minimize cross-entropy $\mathcal{H}(Y; \hat{Y}|Z)$, we implicitly minimize both $\mathcal{H}(Y|Z)$ and $\mathcal{D}_{KL}(Y \parallel \hat{Y}|Z)$. In fact, the optimization could be decoupled into 2 steps in a maximize-minimize (or bound-optimization) way (Boudiaf et al., 2020). The first step fixes the parameters of the network encoder and only minimizes Eq. (10) with respect to the parameters of the network classifier. As this step, $\mathcal{H}(Y|Z)$ is fixed and the predictions \hat{Y} are adjusted to minimize $\mathcal{D}_{KL}(Y \parallel \hat{Y}|Z)$. Ideally, $\mathcal{D}_{KL}(Y \parallel \hat{Y}|Z)$ would vanish at the end of this step (Boudiaf et al., 2020). In this sense, we know that:

$$\mathcal{H}(Y|Z) = \inf \mathcal{H}(Y; \hat{Y}|Z). \quad (11)$$

The second step fixes the classifier and minimizes Eq. (10) with respect to the encoder. By combining Eq. (9) and Eq. (11), we conclude the proof of Theorem 2. \square

B. Pseudo-code of Core-tuning

We summarize the scheme of Core-tuning in Algorithm 1.

Algorithm 1 The training scheme of Core-tuning.

Require: Pre-trained encoder G_e ; Loss factor η ; Mixup factor α ; Batch size B ; Epoch number T ; Threshold $\lambda_p = \lambda_n = 0.8$.

Initialize: Classifier G_y ; Projection head G_c .

```

1: for  $t=1, \dots, T$  do
2:   Sample a batch of training data  $\{(x_i, y_i)\}_{i=1}^B$ ;
3:   Obtain features  $z_i = G_e(x_i)$  for each sample;
4:   for  $i=1, \dots, B$  do
5:     Construct positive pair set  $P_i$  and full pair set  $A_i$  for  $z_i$ ;
6:     Mix hard positive pair  $z_i^+$  and add it to  $P_i, A_i$ ;
7:     Mix hard negative pair  $(z_i^-, y_i^-)$  and add it to  $P_i, A_i$ ;
8:   end for
9:   Obtain contrastive features  $v_i = G_c(z_i)$  for all features;
10:  Compute the focal contrastive loss  $\mathcal{L}_{con}^f$ ;
11:  Predict  $\hat{y}_i = G_y(z_i)$  for original features and hard negatives;
12:  Compute the cross-entropy loss  $\mathcal{L}_{ce}^m$ ;
13:   $\text{loss.backward}()$ ; //  $\text{loss} = \mathcal{L}_{ce}^m + \eta \mathcal{L}_{con}^f$ .
14: end for
    
```

C. More Experimental Details

C.1. Implementation Details of Feature Visualization

In the feature visualization, we train ResNet-18 on CIFAR10 with two kinds of losses, *i.e.*, (1) cross-entropy \mathcal{L}_{ce} ; (2) cross-entropy and the contrastive loss $\mathcal{L}_{ce} + \mathcal{L}_{con}$. For better visualization, following (Liu et al., 2017), we add two fully connected layers before the classifier. The two layers first map the 512-dimensional features to a 3-dimensional feature sphere and then map back to the 10-dimensional feature space for prediction. The contrastive loss \mathcal{L}_{con} is enforced on the 3-dimensional features. After training, we visualize the 3-dimensional features learned by ResNet-18. We implement the feature visualization in MATLAB.

C.2. More Details of Image Classification

Dataset details. Following (Kornblith et al., 2019), we test on 9 natural image datasets, including ImageNet-20 (a subset of ImageNet with 20 classes) (Deng et al., 2009), CIFAR10, CIFAR100 (Krizhevsky et al., 2009), Caltech-101 (Fei-Fei et al., 2004), DTD (Cimpoi et al., 2014), FGVC Aircraft (Maji et al., 2013), Standard Cars (Krause et al., 2013), Oxford-IIIT Pets (Parkhi et al., 2012) and Oxford 102 Flowers (Nilsback & Zisserman, 2008).

Most datasets are obtained from their official websites, except ImageNet-20 and Oxford 102 Flowers. The ImageNet-20 dataset is obtained by combining two open-source ImageNet subsets with 10 classes, *i.e.*, ImageNette and ImageWoof (Howard, 2020). Moreover, Oxford 102 Flowers is obtained from Kaggle¹. These datasets cover a wide range of classification tasks, including coarse-grained ob-

ject classification (*i.e.*, ImageNet-20, CIFAR, Caltech-101), fine-grained object classification (*i.e.*, Cars, Aircraft, Pets) and texture classification (*i.e.*, DTD). The statistics of all datasets are reported in Table 1.

Table 1. Statistics of datasets.

DataSet	#Classes	# Training	# Test
ImageNet-20	20	18,494	7,854
CIFAR10	10	50,000	10,000
CIFAR100	100	50,000	10,000
Caltech-101	102	3,060	6,084
Describable Textures (DTD)	47	3,760	1,880
FGVG Aircraft	100	6,667	3,333
Standard Cars	196	8,144	8,041
Oxford-IIIT Pets	37	3,680	3,369
Oxford 102 Flowers	102	6,552	818

Implementation details. We implement all methods in PyTorch. All checkpoints of contrastive self-supervised models are provided by the authors or by the PyContrast GitHub repository². Since the checkpoints of SimCLR are based on Tensorflow, we convert them to the PyTorch version.

For most datasets, following (Kornblith et al., 2019; Chen et al., 2020), we preprocess images via random resized crops to 224×224 and flips. At the test time, we resize images to 256×256 and then take a 224×224 center crop. In such a preprocessing setting, however, we find it difficult to reproduce the fine-tuning performance of SimCLR, as reported in (Chen et al., 2020). Therefore, for some datasets (*e.g.*, CIFAR10 and Aircraft), we try to resize images to different scales and use rotation augmentations. Although the preprocessing of some datasets is slightly different from (Chen et al., 2020; Zhao et al., 2018; Zhang et al., 2018), the results in this paper are obtained with the same preprocessing method *w.r.t.* each dataset.

Following (Kornblith et al., 2019), we initialize networks with the checkpoints of contrastive self-supervised models. For most datasets except ImageNet-20, we fine-tune networks for 100 epochs at a batch size of 256 using Nesterov momentum. Moreover, we set the initial learning rate to 0.1 and adjust it via the cosine learning rate schedule. For ImageNet-20, we fine-tune networks for 100 epochs at a batch size of 256 using stochastic gradient descent. Besides, we set the initial learning rate to 0.1 and adjust it per 30 epochs via the linear learning rate decay with the factor of 0.1. For all datasets, the momentum parameter is set to 0.9, while the factor of weight decay is set to 10^{-4} . As for Core-tuning, we set thresholds $\lambda_p = \lambda_n = 0.8$ and temperature $\tau = 0.07$ by default. The dimension of the contrastive features is 256. Following (Chen et al., 2020), we perform hyper-parameter tuning for each dataset and select the best ones on a validation set. All results are averaged over 3 runs. We adopt the top-1 accuracy as the metric.

¹<https://www.kaggle.com/c/oxford-102-flower-pytorch>

²<https://github.com/HobbitLong/PyContrast>

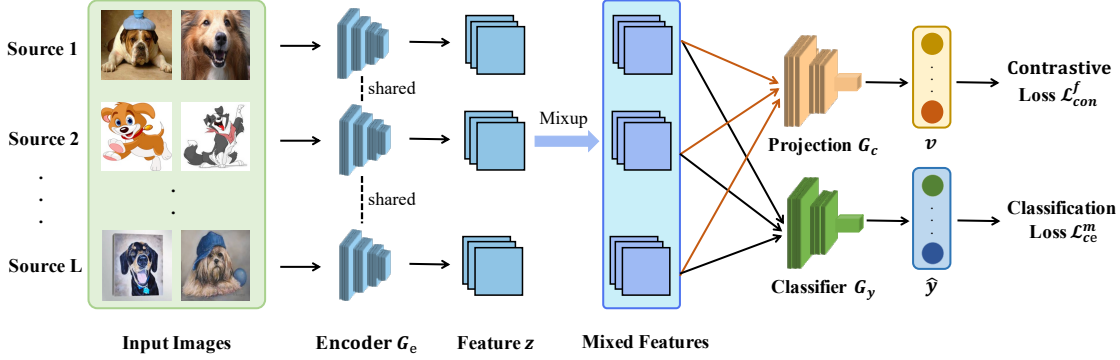


Figure 1. The overall scheme of Core-tuning in the setting of cross-domain generalization. Best viewed in color.

C.3. More Details of Domain Generalization

Dataset details. We use 3 benchmark datasets, *i.e.*, PACS (Li et al., 2017), VLCS (Fang et al., 2013) and Office-Home (Venkateswara et al., 2017). The data statistics are shown in Table 2, where each dataset has 4 domains. In each setting, we select 3 domains to fine-tune the networks and test them on the rest of the unseen domains. The key challenge is the distribution discrepancies among domains, leading to poor performance of neural networks on the target domain (Zhang et al., 2019b; 2020a;b).

Table 2. Statistics of datasets.

DataSet	#Domains	#Classes	#Samples	Size of images
PACS	4	7	9,991	(3,224,224)
VLCS	4	5	10,729	(3,224,224)
Office-Home	4	65	15,588	(3,224,224)

Implementation details. The overall scheme of Core-tuning for domain generalization is shown in Figure 1. The experiments are implemented based on the DomainBed repository (Gulrajani & Lopez-Paz, 2021) in PyTorch. During fine-tuning, we preprocess images through random resized crops to 224×224 , horizon flips, color jitter and random gray scale. At the test time, we directly resize images to 224×224 . We initialize ResNet-50 with the weights of the MoCo-v2 pre-trained model, and fine-tune it for 20,000 steps at a batch size of 32 using the Adam optimizer. We set the initial learning rate to 5×10^{-5} and adjust it via the exponential learning rate decay. All other hyper-parameters of Core-tuning are the same as image classification. Besides, we use Accuracy as the metric in domain generalization.

C.4. More Details of Robustness Training

We conduct this experiment in PyTorch. We take Caltech-101, DTD, Pets, and CIFAR10 as datasets, whose preprocessing are the same as the ones in image classification. We use MoCo-v2 pre-trained ResNet-50 as the backbone. During adversarial training (AT), we use both clean and adversarial samples for training with diverse fine-tuning methods. Other training schemes (*e.g.*, the optimizer, the learning rate scheme) are the same as image classification.

D. More Experimental Results

D.1. More Results on Adversarial Training

In the main paper, we apply Core-tuning to adversarial training on three natural image datasets, *i.e.*, Caltech-101, DTD and Pets. Here, we further apply Core-tuning to CIFAR10. We generate the adversarial samples via Projected Gradient Descent (PGD) (Madry et al., 2018) under ℓ_2 attack (strength $\sigma=0.5$) and ℓ_∞ attack (strength $\sigma=4/255$).

As shown in Table 3, Core-tuning not only achieves better robust accuracy on adversarial samples, but also achieves better clean accuracy on original samples under both ℓ_2 and ℓ_∞ attacks. Such a result is quite promising, since Core-tuning effectively conquers the accuracy-robustness trade-off in adversarial training (Tsipras et al., 2019; Zhang et al., 2019a), which has been found difficult to handle even in the most advanced AT methods (Zhang et al., 2021; Yang et al., 2020).

Table 3. Adversarial training performance of MoCo-v2 pre-trained ResNet-50 on CIFAR10 under the attack of PGD-10 in terms of robust and clean accuracies. CE indicates cross-entropy; AT-CE indicates adversarial training (AT) with CE; AT-CE-Con enhances AT-CE with the contrastive loss; AT-ours uses Core-tuning for AT.

Method	CIFAR10			
	ℓ_2 attack ($\epsilon=0.5$)		ℓ_∞ attack ($\epsilon=4/255$)	
	Robust	Clean	Robust	Clean
CE	50.25 \pm 0.21	94.70 \pm 0.39	12.28 \pm 0.54	94.70 \pm 0.39
AT-CE	86.59 \pm 0.22	92.00 \pm 0.13	75.82 \pm 0.73	91.99 \pm 0.32
AT-CE-Con	90.74 \pm 0.07	94.71 \pm 0.11	79.75 \pm 0.29	93.79 \pm 0.24
AT-ours	92.97\pm0.06	96.82\pm0.06	82.01\pm0.23	95.95\pm0.06

D.2. More Results on Image Classification

In the main paper, we report the results of image classification and ablations studies on 9 natural image datasets in terms of the average accuracy. To make the results more complete, this appendix further reports the results with their standard errors, as shown in Table 4-Table 5.

Table 4. Comparisons of diverse methods for MoCo-v2 pre-trained ResNet-50 model fine-tuning on image classification in terms of top-1 accuracy. Here, “Avg.” indicates the average accuracy over the 9 datasets. SL-CE-tuning denotes supervised pre-training on ImageNet and then fine-tuning with cross-entropy.

Algorithm	ImageNet-20	CIFAR10	CIFAR100	Caltech101	DTD
SL-CE-tuning	91.01+/-1.27	94.23+/-0.07	83.40+/-0.12	93.65+/-0.21	74.40+/-0.45
CE-tuning	88.28+/-0.47	94.70+/-0.39	80.27+/-0.60	91.87+/-0.18	71.68+/-0.53
L2SP (Li et al., 2018)	88.49+/-0.40	95.14+/-0.22	81.43+/-0.22	91.98+/-0.07	72.18+/-0.61
M&M (Zhan et al., 2018)	88.53+/-0.21	95.02+/-0.07	80.58+/-0.19	92.91+/-0.08	72.43+/-0.43
DELTA (Li et al., 2019)	88.35+/-0.41	94.76+/-0.05	80.39+/-0.41	92.19+/-0.45	72.23+/-0.23
BSS (Chen et al., 2019)	88.34+/-0.62	94.84+/-0.21	80.40+/-0.30	91.95+/-0.12	72.22+/-0.17
RIFLE (Li et al., 2020)	89.06+/-0.28	94.71+/-0.13	80.36+/-0.07	91.94+/-0.23	72.45+/-0.30
SCL (Gunel et al., 2021)	89.29+/-0.07	95.33+/-0.09	81.49+/-0.27	92.84+/-0.03	72.73+/-0.31
Bi-tuning (Zhong et al., 2021)	89.06+/-0.08	95.12+/-0.15	81.42+/-0.01	92.83+/-0.06	73.53+/-0.37
Core-tuning	92.59+/-0.09	97.31+/-0.10	84.13+/-0.27	93.46+/-0.06	75.37+/-0.37

Algorithm	Aircraft	Cars	Pets	Flowers	Avg.
SL-CE-tuning	87.03+/-0.02	89.77+/-0.11	92.17+/-0.12	98.78+/-0.10	89.35
CE-tuning	86.87+/-0.18	88.61+/-0.43	89.05+/-0.01	98.49+/-0.06	87.76
L2SP (Li et al., 2018)	86.55+/-0.30	89.00+/-0.23	89.43+/-0.27	98.66+/-0.20	88.10
M&M (Zhan et al., 2018)	87.45+/-0.28	88.90+/-0.70	89.60+/-0.09	98.57+/-0.15	88.22
DELTA (Li et al., 2019)	87.05+/-0.37	88.73+/-0.05	89.54+/-0.48	98.65+/-0.17	87.99
BSS (Chen et al., 2019)	87.18+/-0.71	88.50+/-0.02	89.50+/-0.42	98.57+/-0.15	87.94
RIFLE (Li et al., 2020)	87.60+/-0.50	89.72+/-0.11	90.05+/-0.26	98.70+/-0.06	88.29
SCL (Gunel et al., 2021)	87.44+/-0.31	89.37+/-0.13	89.71+/-0.20	98.65+/-0.10	88.54
Bi-tuning (Zhong et al., 2021)	87.39+/-0.01	89.41+/-0.28	89.90+/-0.06	98.57+/-0.10	88.58
Core-tuning	89.48+/-0.17	90.17+/-0.03	92.36+/-0.14	99.18+/-0.15	90.45

Table 5. Ablation studies of Core-tuning (Row 5) for fine-tuning MoCo-v2 pre-trained ResNet-50 on 9 natural image datasets in terms of top-1 accuracy. Here, “Avg.” indicates the average accuracy over the 9 datasets. Besides, \mathcal{L}_{con} is the original supervised contrastive loss, while \mathcal{L}_{con}^f is our focal contrastive loss. Moreover, “mixup” denotes the manifold mixup, while “mixup-hard” indicates the proposed feature mixup strategy in our method.

\mathcal{L}_{ce}	\mathcal{L}_{con}	\mathcal{L}_{con}^f	mixup	mixup-hard	ImageNet-20	CIFAR10	CIFAR100	Caltech101	DTD
✓					88.28+/-0.47	94.70+/-0.39	80.27+/-0.60	91.87+/-0.18	71.68+/-0.53
✓	✓				89.29+/-0.07	95.33+/-0.09	81.49+/-0.27	92.84+/-0.03	72.73+/-0.31
✓			✓		90.67+/-0.09	95.43+/-0.20	81.03+/-0.11	92.68+/-0.06	73.31+/-0.40
✓	✓			✓	92.20+/-0.15	97.01+/-0.10	83.89+/-0.20	93.22+/-0.18	74.78+/-0.31
✓		✓		✓	92.59+/-0.09	97.31+/-0.10	84.13+/-0.27	93.46+/-0.06	75.37+/-0.37

\mathcal{L}_{ce}	\mathcal{L}_{con}	\mathcal{L}_{con}^f	mixup	mixup-hard	Aircraft	Cars	Pets	Flowers	Avg.
✓					86.87+/-0.18	88.61+/-0.43	89.05+/-0.01	98.49+/-0.06	87.76
✓	✓				87.44+/-0.31	89.37+/-0.13	89.71+/-0.20	98.65+/-0.10	88.54
✓			✓		88.37+/-0.14	89.06+/-0.14	91.37+/-0.03	98.74+/-0.11	88.96
✓	✓			✓	88.88+/-0.34	89.79+/-0.12	91.95+/-0.33	98.94+/-0.12	90.07
✓		✓		✓	89.48+/-0.17	90.17+/-0.03	92.36+/-0.14	99.18+/-0.15	90.45

D.3. Analysis of Projection Dimension and Depth

In previous experiments, we use a 2-layer MLP to extract contrastive features with the dimension 256. Here, we further analyze how the dimension and the depth influence Core-tuning. The results on ImageNet-20 are reported in Figure 2, where the fine-tuning performance of Core-tuning can be further improved by changing the feature dimension to 128 and the depth to 3. Note that the best dimension and depth of the projection head may vary on different datasets, but the default setting (*i.e.*, dimension 256 and depth 2) is enough to obtain consistently good performance.

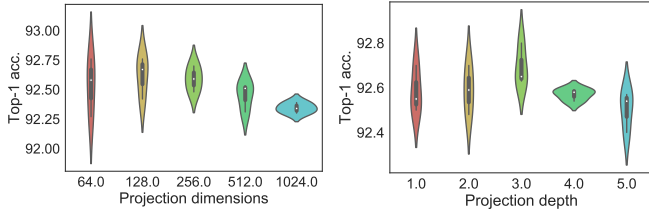


Figure 2. Sensitivity analysis of the projection dimension and the projection depth in Core-tuning on ImageNet-20 based on MoCo-v2 pre-trained ResNet-50. Each run tests one parameter and fixes others. Best viewed in color.

D.4. Analysis of Temperature Factor

Following the implementation of the supervised contrastive loss (Khosla et al., 2020), we set the temperature factor τ to 0.07 for Core-tuning by default. In this section, we further analyze the influence of τ on Core-tuning when fine-tuning MoCo-v2 pre-trained models on ImageNet-20. As shown in Figure 3, when τ is small (*e.g.*, 0.01 or 0.07), Core-tuning performs slightly better on ImageNet-20. The potential reason is that a small temperature parameter implicitly helps the method to learn hard positive/negative pairs (Wang & Liu, 2020), which are more informative and beneficial to contrastive learning. Note that the best τ can be different on different datasets, but the default setting (*i.e.*, $\tau = 0.07$) is enough to achieve comparable performance.

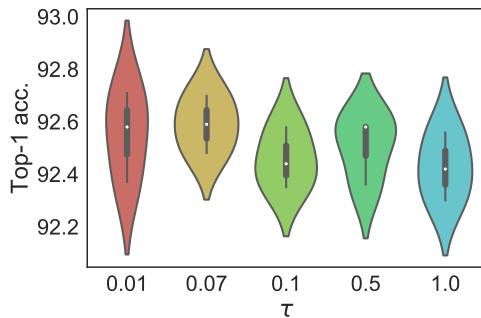


Figure 3. Sensitivity analysis of the temperature factor in Core-tuning on the ImageNet-20 dataset based on the MoCo-v2 pre-trained ResNet-50 model. Best viewed in color.

D.5. Relationship Between Pre-training and Fine-tuning Accuracies

We further explore the relationship between ImageNet performance and Core-tuning fine-tuning performance on Caltech-101 for diverse contrastive self-supervised models. Here, the ImageNet performance of a contrastive self-supervised model is obtained by training a new linear classifier on the frozen pre-trained representation and then evaluate the model on the ImageNet test set. For convenience, we directly follow the ImageNet performance reported in the original paper of the corresponding methods.

As shown in Figure 4, the fine-tuning result of each contrastive self-supervised model on Caltech-101 is highly correlated with the model result on ImageNet. This implies that the ImageNet performance can be a good predictor for the fine-tuning performance of contrastive self-supervised models. Such a finding is consistent with supervised pre-trained models (Kornblith et al., 2019). Even so, note that the correlation is not perfect, where a contrastive pre-trained model with better ImageNet performance does not necessarily mean better fine-tuning performance, *e.g.*, SimCLR-v2 vs MoCo-v2.

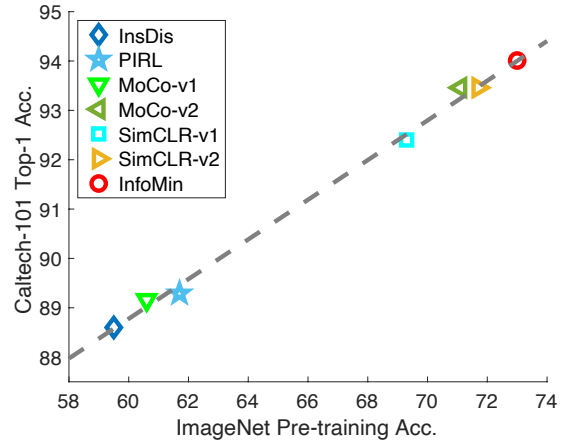


Figure 4. The relationship between ImageNet performance and Core-tuning fine-tuning performance on Caltech-101 for contrastive self-supervised ResNet-50 models. Better viewed in color.

References

- Boudiaf, M., Rony, J., et al. A unifying mutual information view of metric learning: cross-entropy vs. pairwise losses. In *European Conference on Computer Vision*, 2020.
- Chen, T., Kornblith, S., Norouzi, M., and Hinton, G. A simple framework for contrastive learning of visual representations. In *International Conference on Machine Learning*, 2020.
- Chen, X., Wang, S., et al. Catastrophic forgetting meets negative transfer: Batch spectral shrinkage for safe transfer learning. In *Advances in Neural Information Processing Systems*, 2019.

- Cimpoi, M., Maji, S., Kokkinos, I., Mohamed, S., and Vedaldi, A. Describing textures in the wild. In *Computer Vision and Pattern Recognition*, pp. 3606–3613, 2014.
- Deng, J., Dong, W., Socher, R., Li, L.-J., Li, K., and Fei-Fei, L. Imagenet: A large-scale hierarchical image database. In *Computer Vision and Pattern Recognition*, pp. 248–255, 2009.
- Fang, C., Xu, Y., et al. Unbiased metric learning: On the utilization of multiple datasets and web images for softening bias. In *International Conference on Computer Vision*, 2013.
- Fei-Fei, L., Fergus, R., and Perona, P. Learning generative visual models from few training examples: An incremental bayesian approach tested on 101 object categories. In *Computer Vision and Pattern Recognition Workshop*, 2004.
- Gulrajani, I. and Lopez-Paz, D. In search of lost domain generalization. In *International Conference on Learning Representations*, 2021.
- Gunel, B., Du, J., Conneau, A., and Stoyanov, V. Supervised contrastive learning for pre-trained language model fine-tuning. In *International Conference on Learning Representations*, 2021.
- Howard, J. The imagenette and imagewoof datasets, 2020. URL <https://github.com/fastai/imagenette/>.
- Khosla, P., Teterwak, P., et al. Supervised contrastive learning. In *Advances in Neural Information Processing Systems*, 2020.
- Kornblith, S., Shlens, J., and Le, Q. V. Do better imagenet models transfer better? In *Computer Vision and Pattern Recognition*, pp. 2661–2671, 2019.
- Krause, J., Deng, J., Stark, M., and Fei-Fei, L. Collecting a large-scale dataset of fine-grained cars. 2013.
- Krizhevsky, A., Hinton, G., et al. Learning multiple layers of features from tiny images. 2009.
- Li, D., Yang, Y., Song, Y.-Z., and Hospedales, T. M. Deeper, broader and artier domain generalization. In *International Conference on Computer Vision*, pp. 5542–5550, 2017.
- Li, X., Grandvalet, Y., and Davoine, F. Explicit inductive bias for transfer learning with convolutional networks. In *International Conference on Machine Learning*, 2018.
- Li, X., Xiong, H., et al. Delta: Deep learning transfer using feature map with attention for convolutional networks. In *International Conference on Learning Representations*, 2019.
- Li, X., Xiong, H., et al. Rifle: Backpropagation in depth for deep transfer learning through re-initializing the fully-connected layer. In *International Conference on Machine Learning*, 2020.
- Liu, W., Wen, Y., Yu, Z., Li, M., Raj, B., and Song, L. Sphereface: Deep hypersphere embedding for face recognition. In *Computer Vision and Pattern Recognition*, pp. 212–220, 2017.
- Madry, A., Makelov, A., Schmidt, L., Tsipras, D., and Vladu, A. Towards deep learning models resistant to adversarial attacks. In *International Conference on Learning Representations*, 2018.
- Maji, S., Rahtu, E., Kannala, J., Blaschko, M., and Vedaldi, A. Fine-grained visual classification of aircraft. *ArXiv*, 2013.
- Nilsback, M.-E. and Zisserman, A. Automated flower classification over a large number of classes. In *Indian Conference on Computer Vision, Graphics & Image Processing*, 2008.
- Parkhi, O. M., Vedaldi, A., Zisserman, A., and Jawahar, C. Cats and dogs. In *Computer Vision and Pattern Recognition*, 2012.
- Tsipras, D., Santurkar, S., Engstrom, L., Turner, A., and Madry, A. Robustness may be at odds with accuracy. In *International Conference on Learning Representations*, 2019.
- Venkateswara, H., Eusebio, J., Chakraborty, S., and Panchanathan, S. Deep hashing network for unsupervised domain adaptation. In *Computer Vision and Pattern Recognition*, 2017.
- Wang, F. and Liu, H. Understanding the behaviour of contrastive loss. *Arxiv*, 2020.
- Wang, M. and Sha, F. Information theoretical clustering via semidefinite programming. In *International Conference on Artificial Intelligence and Statistics*, pp. 761–769, 2011.
- Wen, Y., Zhang, K., Li, Z., and Qiao, Y. A discriminative feature learning approach for deep face recognition. In *European Conference on Computer Vision*, pp. 499–515, 2016.
- Yang, Y.-Y., Rashtchian, C., Zhang, H., Salakhutdinov, R., and Chaudhuri, K. A closer look at accuracy vs. robustness. In *Advances in Neural Information Processing Systems*, 2020.
- Zhan, X., Liu, Z., Luo, P., Tang, X., and Loy, C. C. Mix-and-match tuning for self-supervised semantic segmentation. In *AAAI Conference on Artificial Intelligence*, 2018.
- Zhang, H., Yu, Y., Jiao, J., Xing, E., El Ghaoui, L., and Jordan, M. Theoretically principled trade-off between robustness and accuracy. In *International Conference on Machine Learning*, 2019a.
- Zhang, J., Zhu, J., Niu, G., Han, B., Sugiyama, M., and Kankanhalli, M. Geometry-aware instance-reweighted adversarial training. In *International Conference on Learning Representations*, 2021.
- Zhang, Y., Zhao, P., et al. Online adaptive asymmetric active learning for budgeted imbalanced data. In *ACM SIGKDD International Conference on Knowledge Discovery & Data Mining*, pp. 2768–2777, 2018.
- Zhang, Y., Chen, H., et al. From whole slide imaging to microscopy: Deep microscopy adaptation network for histopathology cancer image classification. In *International Conference on Medical Image Computing and Computer-Assisted Intervention*, pp. 360–368, 2019b.
- Zhang, Y., Niu, S., et al. Covid-da: Deep domain adaptation from typical pneumonia to covid-19. *arXiv*, 2020a.
- Zhang, Y., Wei, Y., et al. Collaborative unsupervised domain adaptation for medical image diagnosis. *IEEE Transactions on Image Processing*, 2020b.
- Zhao, P., Zhang, Y., Wu, M., Hoi, S. C., Tan, M., and Huang, J. Adaptive cost-sensitive online classification. *IEEE Transactions on Knowledge and Data Engineering*, 2018.
- Zhong, J., Wang, X., Kou, Z., Wang, J., and Long, M. Bi-tuning of pre-trained representations. *Submission to International Conference on Learning Representations*, 2021.